J|A|C|S
ARTICLES
Published on Web 11/23/2002

Responsive Hydrogels from the Intramolecular Folding and Self-Assembly of a Designed Peptide

Joel P. Schneider,*,† Darrin J. Pochan,*,‡ Bulent Ozbas, Karthikan Rajagopal, Lisa Pakstis, and Juliana Kretsinger

Contribution from the Departments of Chemistry and Biochemistry and Materials Science and Engineering and the Delaware Biotechnology Institute, University of Delaware, Newark, Delaware 19716

Received August 2, 2002

Abstract: A general peptide design is presented that links the pH-dependent intramolecular folding of β-hairpin peptides to their propensity to self-assemble, affording hydrogels rich in β-sheet. Chemical responsiveness has been specifically engineered into the material by linking intramolecular folding to changes in solution pH, and mechanical responsiveness, by linking hydrogelation to self-assembly. Circular dichroic and infrared spectroscopies show that at low pH individual peptides are unstructured, affording a low-viscosity aqueous solution. Under basic conditions, intramolecular folding takes place, affording amphiphilic β-hairpins that intermolecularly self-assemble. Rheology shows that the resulting hydrogel is rigid but is shear-thinning. However, quick mechanical strength recovery after cessation of shear is observed due to the inherent self-assembled nature of the scaffold. Characterization of the gelation process, from the molecular level up through the macroscopic properties of the material, suggests that by linking the intramolecular folding of small designed peptides to their ability to self-assemble, responsive materials can be prepared. Cryo-transmission electron and laser scanning confocal microscopies reveal a water-filled porous scaffold on both the nano- and microscale. The environmental responsiveness, morphology, and peptidic nature make this hydrogel a possible material candidate for biomedical and engineering technology.

The preparation of materials via molecular self-assembly allows one to define ultimate material properties by careful design of the individual constituent molecules. Characteristics such as chemical functionality, material morphology, mechanical/viscoelastic properties, and consequent processibility can be designed for at the molecular level. Using peptides as the molecular building blocks for self-assembly not only offers the possibility of incorporating biofunctionality (ligand and metal recognition, biocompatibility, and biodegradability) into the material but also offers the exciting possibility of linking intramolecular peptide folding to material characteristics. Reported here is a hydrogelation system that is defined by the intramolecular folding and consequent self-assembly of a monomeric peptide. Importantly, this peptide is designed such that the ultimate material properties are responsive to this intramolecular folding event.

Hydrogels, a class of materials integral to biotechnologies such as tissue engineering/drug delivery[1] and microfluidics,[2] are classically made from high molecular weight natural polymers such as gelatin,[3] fibrin,[4] and polysaccharide-derived polymers,[5] as well as from synthetic molecules such as polymers of acrylic acid, ethylene oxide, vinyl alcohol, and derivatives thereof.[6] An alternative approach is the use of proteinaceous polymers in which the molecular tools afforded by proteins can be exploited (e.g., secondary and tertiary structure, biofunctionality, biocompatibility, and enzymatic biodegradability). Large pure protein polymers synthesized by chemical polymerization,[7] or more commonly by recombinant DNA techniques, have been used to prepare hydrogels,[8,9] some of which are environmentally responsive to pH and temperature.[8,10,11]

We are interested in an alternate strategy that employs small peptides for the preparation of responsive hydrogels. These gels are constructed via a pure self-assembly mechanism that eliminates the need for exogenous cross-linking agents. Instead, we take advantage of the intramolecular folding propensity of a class of peptides known as β-hairpins not only to drive self-

* Corresponding authors: e-mail schneijp@udel.edu or pochan@udel.edu.
† Department of Chemistry and Biochemistry.
‡ Department of Materials Science and Engineering and Delaware Biotechnology Institute.

(1) Lee, K. Y.; Mooney, D. J. *Chem. Rev.* **2001**, *101*, 1869−1879.
(2) Beebe, D. J.; Moore, J. S.; Bauer, J. M.; Yu, Q.; Liu, R. H.; Devadoss, C.; Jo, B. H. *Nature* **2000**, *404*, 588.
(3) Kavanagh, G. M.; Ross-Murphy, S. B. *Prog. Polym. Sci.* **1998**, *23*, 533−562.
(4) Perka, C.; Spitzer, R. S.; Lindenhayn, K.; Sittinger, M.; Schultz, O. *J. Biomed. Mater. Res.* **2000**, *49*, 305−311.
(5) Chenite, A.; Chaput, C.; Wang, D.; Combes, C.; Buschmann, M. D.; Hoemann, C. D.; Leroux, J. C.; Atkinson, B. L.; Binette, F.; Selmani, A. *Biomaterials* **2000**, *21*, 2155−2161.
(6) Peppas, N. A.; Bures, P.; Leobandung, W.; Ichikawa, H. *Eur. J. Pharm. Biopharm.* **2000**, *50*, 27−46.
(7) Nowak, A. P.; Breedveld, V.; Pakstis, L.; Ozbas, B.; Pine, D. J.; Pochan, D.; Deming, T. J. *Nature* **2002**, *417*, 424−428.
(8) Petka, W. A.; Harden, J. L.; McGrath, K. P.; Wirtz, D.; Tirrell, D. A. *Science* **1998**, *281*, 389−392.
(9) Qu, Y.; Payne, S. C.; Apkarian, R. P.; Conticello, V. P. *J. Am. Chem. Soc.* **2000**, *122*, 5014−5015.
(10) Lee, J.; Macosko, C. W.; Urry, D. W. *Macromolecules* **2001**, *34*, 4114−4123.
(11) McMillan, R. A.; Conticello, V. P. *Macromolecules* **2000**, *33*, 4809−4821.

10.1021/ja027993g CCC: $22.00

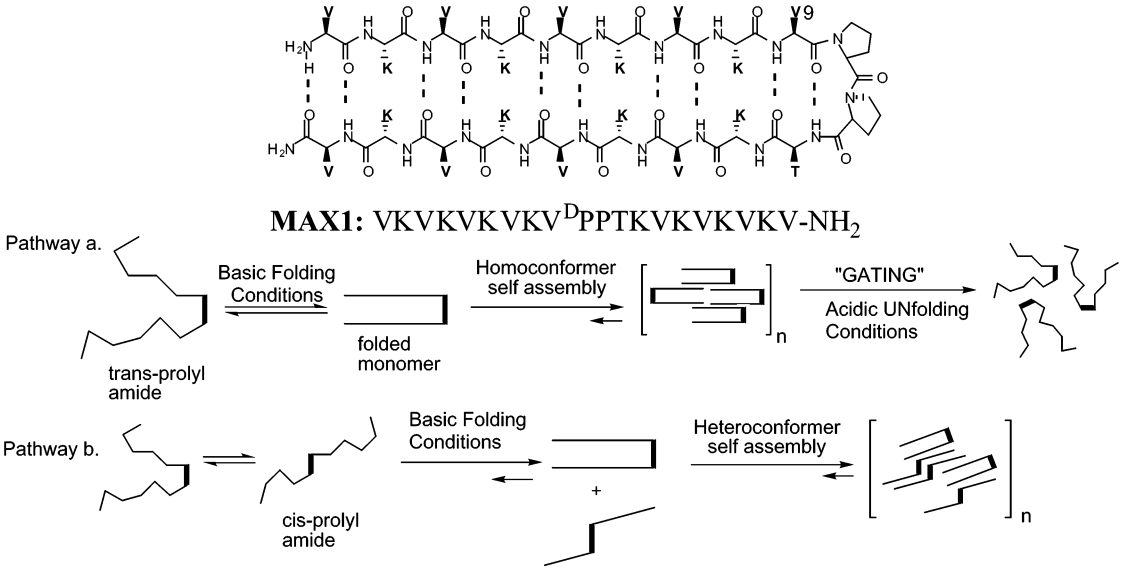

Figure 1. Sequence and proposed β-hairpin structure of MAX1. Alternate folding/self-assembly pathways dependent on turn structure contained within MAX1. Valine at position 9 strongly enforces a *trans*-prolyl amide bond geometry favoring hairpin formation prior to self-assembly (pathway a). A cis geometry, which is designed against, may result in an extended conformation which could undergo mixed self-assembly with correctly folded hairpins (pathway b).

assembly leading to hydrogel formation but also as a vehicle to introduce environmental responsiveness. In general, the preparation of materials from small peptides is advantageous because peptides can be quickly chemically synthesized and novel amino acid residues can be readily incorporated. In addition, the use of orthogonal protection strategies allows for regioselective ligation of chemical moieties to amino acid side chains, affording conjugates with tailored functions. In terms of regioselectivity, the ability to completely and precisely functionalize the monomeric building block of a self-assembling system is highly desirable when compared to the relatively nonselective methods used to chemically modify an existing polymer.

While examples exist of ornate peptide-derived conjugates that self-assemble into hydrogels,[12,13] the ability of small, simple peptides to form materials of equal or greater complexity is intriguing. For example, researchers have studied small peptides and peptidomimetics that intermolecularly self-assemble into sheet-rich hydrogels[14−20] and other supramolecular structures.[21−37] These examples demonstrate that molecular architects employing peptides as construction material can build complex static and functional structures. Described here is a peptide-based self-assembly system in which form follows function.

Figure 1 shows a designed, fully reversible self-assembly mechanism that links intramolecular folding to self-assembly. This system entails the use of a designed peptide that can *not* self-assemble until controlled solution conditions (aqueous solutions buffered at pH 9) permit intramolecular folding of the peptide into a β-hairpin conformation. This folded state is prone to self-assembly, affording environmentally sensitive hydrogels characterized by rigid gel networks ($G' > 1$ kPa). Importantly, the hydrogel is responsive to both mechanical and chemical stimuli. Due to the hydrogel's self-assembled nature, gel strength quickly recovers after the material experiences any amount of shear. In addition, since the unimolecular folding event that results in gelation is a reversible process governed by pH, simple acidification of the solution results in β-hairpin unfolding with consequent hydrogel dissolution. *Thus, the intramolecular folding of a small peptide on the nanoscale is used to control macroscopic material properties.*

(12) Sanborn, T. J.; Messersmith, P. B.; Barron, A. E. *Biomaterials* **2002**, *23*, 2703−2710.
(13) Hartgerink, J. D.; Beniash, E.; Stupp, S. I. *Proc. Natl. Acad. Sci. U.S.A.* **2002**, *99*, 5133−5138.
(14) Zhang, S. G.; Lockshin, C.; Cook, R.; Rich, A. *Biopolymers* **1994**, *34*, 663−672.
(15) Caplan, M. R.; Moore, P. N.; Zhang, S. G.; Kamm, R. D.; Lauffenburger, D. A. *Biomacromolecules* **2000**, *1*, 627−631.
(16) Holmes, T. C.; de Lacalle, S.; Su, X.; Liu, G. S.; Rich, A.; Zhang, S. G. *Proc. Natl. Acad. Sci. U.S.A.* **2000**, *97*, 6728−6733.
(17) Collier, J. H.; Hu, B. H.; Ruberti, J. W.; Zhang, J.; Shum, P.; Thompson, D. H.; Messersmith, P. B. *J. Am. Chem. Soc.* **2001**, *123*, 9463−9464.
(18) Aggeli, A.; Bell, M.; Boden, N.; Keen, J. N.; Knowles, P. F.; McLeish, T. C. B.; Pitkeathly, M.; Radford, S. E. *Nature* **1997**, *386*, 259−262.
(19) Gay, N. J.; Packman, L. C.; Weldon, M. A.; Barna, J. C. J. *FEBS Lett.* **1991**, *291*, 87−91.
(20) Holmes, T. C. *Trends Biotechnol.* **2002**, *20*, 16−21.
(21) Marini, D. M.; Hwang, W.; Lauffenburger, D. A.; Zhang, S. G.; Kamm, R. D. *Nano Lett.* **2002**, *2*, 295−299.
(22) Vauthey, S.; Santoso, S.; Gong, H. Y.; Watson, N.; Zhang, S. G. *Proc. Natl. Acad. Sci. U.S.A.* **2002**, *99*, 5355−5360.
(23) Brown, C. L.; Aksay, I. A.; Saville, D. A.; Hecht, M. H. *J. Am. Chem. Soc.* **2002**, *124*, 6846−6848.
(24) Xu, G. F.; Wang, W. X.; Groves, J. T.; Hecht, M. H. *Proc. Natl. Acad. Sci. U.S.A.* **2001**, *98*, 3652−3657.
(25) Rapaport, H.; Kjaer, K.; Jensen, T. R.; Leiserowitz, L.; Tirrell, D. A. *J. Am. Chem. Soc.* **2000**, *122*, 12523−12529.
(26) Bong, D. T.; Ghadiri, M. R. *Angew. Chem., Int. Ed.* **2001**, *40*, 2163−2166.
(27) Bong, D. T.; Clark, T. D.; Granja, J. R.; Ghadiri, M. R. *Angew. Chem., Int. Ed.* **2001**, *40*, 988−1011.
(28) Clark, T. D.; Buriak, J. M.; Kobayashi, K.; Isler, M. P.; McRee, D. E.; Ghadiri, M. R. *J. Am. Chem. Soc.* **1998**, *120*, 8949−8962.
(29) Rapaport, H.; Kim, H. S.; Kjaer, K.; Howes, P. B.; Cohen, S.; Als-Nielsen, J.; Ghadiri, M. R.; Leiserowitz, L.; Lahav, M. *J. Am. Chem. Soc.* **1999**, *121*, 1186−1191.
(30) Kirschner, D. A.; Inouye, H.; Duffy, L. K.; Sinclair, A.; Lind, M.; Selkoe, D. J. *Proc. Natl. Acad. Sci. U.S.A.* **1987**, *84*, 6953−6957.
(31) Lashuel, H. A.; LaBrenz, S. R.; Woo, L.; Serpell, L. C.; Kelly, J. W. *J. Am. Chem. Soc.* **2000**, *122*, 5262−5277.
(32) Choo, D. W.; Schneider, J. P.; Graciani, N. R.; Kelly, J. W. *Macromolecules* **1996**, *29*, 355−366.
(33) Bekele, H.; Fendler, J. H.; Kelly, J. W. *J. Am. Chem. Soc.* **1999**, *121*, 7266−7267.
(34) Powers, E. T.; Kelly, J. W. *J. Am. Chem. Soc.* **2001**, *123*, 775−776.
(35) Das, G.; Ouali, L.; Adrian, M.; Baumeister, B.; Wilkinson, K. J.; Matile, S. *Angew. Chem., Int. Ed.* **2001**, *40*, 4657-+.
(36) Janek, K.; Behlke, J.; Zipper, J.; Fabian, H.; Georgalis, Y.; Beyermann, M.; Bienert, M.; Krause, E. *Biochemistry* **1999**, *38*, 8246−8252.
(37) Cubberley, M. S.; Iverson, B. L. *Curr. Opin. Chem. Biol.* **2001**, *5*, 650−653.

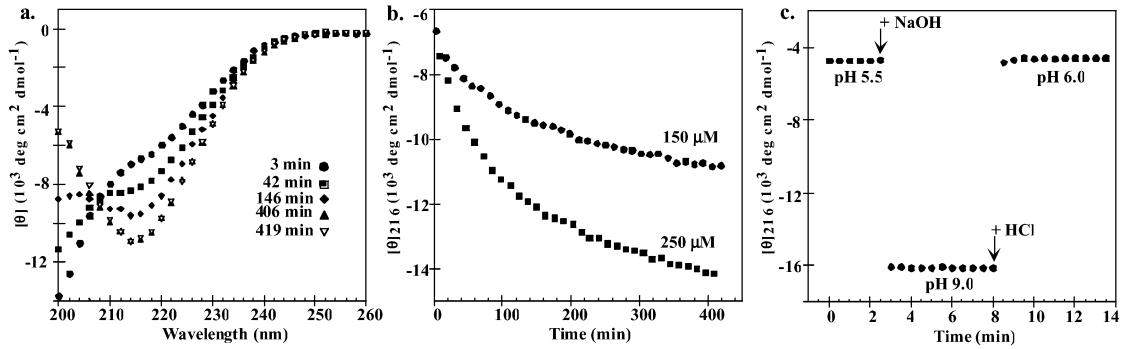

Figure 2. (a) Time-dependent far UV−CD spectra of an unstirred 150 μM MAX1 solution (pH 9.0, 125 mM borate and 10 mM NaCl). (b) $[\theta]_{216}$ monitored as a function of time for unstirred 150 and 250 μM solutions of MAX1 under identical conditions. (c) $[\theta]_{216}$ monitored as a function of time and pH for a stirred 300 μM solution of MAX1 showing that the random coil−sheet folding/self-assembly equilibria are reversible.

Results and Discussion

Peptide Design. MAX1, a 20-residue peptide, is designed to adopt β-hairpin secondary structure via a pH-promoted intramolecular folding event. The sequence is composed of high β-sheet propensity valine and lysine residues[38−40] flanking an intermittent tetrapeptide (-V^{D}PPT-) designed to adopt type II′ turn structure (Figure 1).[41−43] In addition to incorporating local design elements to stabilize hairpin structure, nonlocal effects were also considered by arranging the polar and apolar residues flanking the β-turn in an alternating fashion to favor β-hairpin formation in the self-assembled state.[44] Interestingly, this design seemingly contradicts previous literature that states that peptides composed exclusively of alternating positively charged and hydrophobic residues only form disordered precipitates and not organized gel scaffolds.[16] However, MAX1 clearly self-associates without precipitating and seems to indicate that these limitations in sequence can be circumvented by appropriately designing peptides for the controlled presentation of amphiphilicity.

The ability of MAX1 to assemble is dependent upon its unimolecular folded state. Under basic aqueous solution conditions, where some of the lysine side chains of MAX1 are neutral, this peptide intramolecularly folds into an amphiphilic β-hairpin where one face of the hairpin is lined with hydrophobic valine residues and the other face is lined with hydrophilic lysine residues. After intramolecular folding, subsequent self-assembly of monomeric hairpins is facilitated both laterally via H-bond formation between distinct hairpins and facially by hydrophobic association of the valine-rich faces of folded peptide. Importantly, unimolecular folding is designed to be reversible. Lowering the pH below the intrinsic pK_a of the lysine side chains results in intrastrand charge repulsion from neighboring lysines and subsequent unfolding of individual hairpins, ultimately gating the self-assembled hydrogel structure (Figure 1, pathway a). This simple but effective folding/unfolding trigger is based on the observation that peptidomimetics designed by Kelly and co-workers,[45,46] incorporating similar sequences, have been shown to fold in a pH-dependent manner.

In addition to the design elements discussed above, a β-branched residue was placed at the *i* position of the turn (Val-9) to enforce a *trans*-prolyl amide bond geometry at the $i + 1$ position.[47,48] This key design element ensures that under folding conditions, intramolecular folding of monomeric hairpins is favored *prior* to self-assembly (Figure 1, pathway a). A *cis*-prolyl bond, which is designed against, could result in the presentation of individual β-strands within each monomer in an extended conformation. Peptides capable of adopting both cis and trans conformers could undergo indiscriminant self-association of extended and intramolecularly folded monomers (Figure 1, pathway b). Although aggregation from unfolded peptide leading to hydrogelation cannot be ruled out, it is actively designed against. Thorough characterization of the gelation process from the molecular level up through the macroscopic properties of the material indicates that, by linking the intramolecular folding of MAX1 to its ability to self-assemble, a responsive material can be prepared.

Circular Dichroic Spectroscopy. Time-dependent CD studies support the proposed mechanism of self-assembly. Figure 2a shows that at low micromolar concentrations, unstirred solutions of MAX1 undergo a random coil to β-sheet transition taking hours when the pH is increased from 5.5 (unfolding conditions) to 9.0 (folding conditions). The CD spectrum at 406 min displays a clear minimum at 216 nm, indicating that MAX1 adopts a structure rich in β-sheet.[49] The fact that CD spectra of basic unstirred solutions of this peptide display contributions from random coil signal even after several hours suggests that this peptide undergoes reversible unimolecular folding and unfolding, which is rapid, and that the rate-limiting step in gelation is the self-association event (Figure 1, pathway a). The random coil−sheet transition of monomeric *de novo* designed hairpins and three-stranded antiparallel sheets are known to occur with rates in the microsecond time regime.[50,51]

Figure 2b demonstrates that the observed θ_{216} is concentration-dependent (comparing θ_{216} at any one time point for both concentrations), indicating that MAX1 is self-associating and

(38) Kim, C. A.; Berg, J. M. *Nature* **1993**, *362*, 267−70.
(39) Minor, D. L., Jr.; Kim, P. S. *Nature* **1994**, *367*, 660−3.
(40) Brack, A.; Orgel, L. E. *Nature* **1975**, *256*, 383−387.
(41) Nair, C. M.; Vijayan, M.; Venkatachalapathi, Y. V.; Balaram, P. *J. Chem. Soc., Chem. Commun.* **1979**, 1183−1184.
(42) Bean, J. W.; Kopple, K. D.; Peishoff, C. E. *J. Am. Chem. Soc.* **1992**, *114*, 5328−5334.
(43) Stanger, H. E.; Gellman, S. H. *J. Am. Chem. Soc.* **1998**, *120*, 4236−4237.
(44) Xiong, H. Y.; Buckwalter, B. L.; Shieh, H. M.; Hecht, M. H. *Proc. Natl. Acad. Sci. U.S.A.* **1995**, *92*, 6349−6353.
(45) Nesloney, C. L.; Kelly, J. W. *J. Am. Chem. Soc.* **1996**, *118*, 5836−5845.
(46) Diaz, H.; Tsang, K. Y.; Choo, D.; Kelly, J. W. *Tetrahedron* **1993**, *49*, 3533−3545.
(47) Grathwohl, C.; Wuthrich, K. *Biopolymers* **1976**, *15*, 2025−2041.
(48) Struthers, M. D.; Cheng, R. P.; Imperiali, B. *J. Am. Chem. Soc.* **1996**, *118*, 3073−3081.
(49) Johnson, W. C. *Proteins: Struct., Funct., Genet.* **1990**, *7*, 205−214.
(50) de Alba, E.; Santoro, J.; Rico, M.; Jimenez, M. A. *Protein Sci.* **1999**, *8*, 854−865.
(51) Munoz, V.; Thompson, P. A.; Hofrichter, J.; Eaton, W. A. *Nature* **1997**, *390*, 196−199.

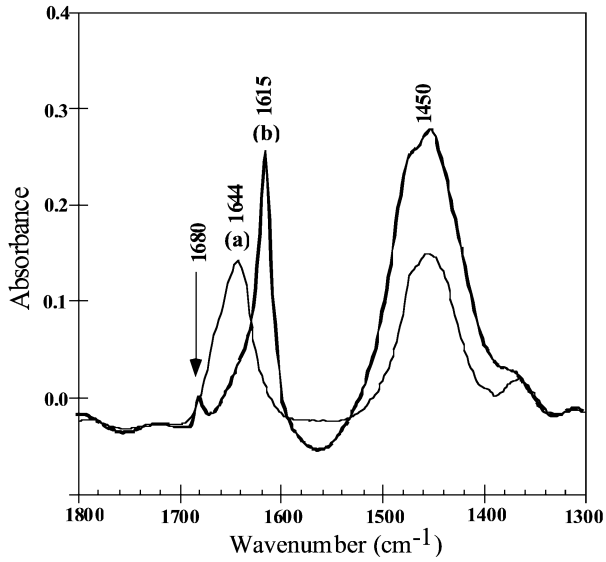

Figure 3. FTIR of 1 wt % MAX1 in D2O at pH 5.5, where the peptide is soluble (trace a), and pH 9.0, after gelation occurs (trace b). A shift in the amide I band from 1644 to 1615 cm^{-1} indicates that the peptide adopts a structure rich in β-sheet upon hydrogel formation.

that the rate of assembly increases as the concentration increases. This behavior is consistent across all spectro- and microscopic methods used to interrogate MAX1. For example, at low micromolar concentrations used for the CD studies shown in Figure 2a,b, self-assembly takes hours. At millimolar concentrations, such as those used in the rheological studies, self-assembly leading to hydrogel takes minutes.

Interestingly, the rate of sheet formation as assessed by CD not only is concentration-dependent but also depends on the rate of mixing; vigorously stirred samples adopt sheet structure faster (within seconds). However, for preparative-scale formulation of MAX1-derived hydrogels, minimally agitated solutions of peptide lead to more uniform gels.

The reversibility of the self-assembly process was investigated by measuring θ_{216} as a function of pH and time as shown in Figure 2c. A stirred solution of MAX1 at pH 5.5 exists as an ensemble of random coil conformations. Adjusting the pH to 9.0 by the addition of NaOH results in β-sheet formation as expected. However, subsequent adjustment of the pH to 6.0 results in a complete loss of sheet signal and full recovery of random coil signal. This experiment demonstrates that the self-assembly process is reversible, presumably as a consequence of deprotonating and reprotonating the lysine side chains, resulting in unimolecular folding and unfolding of MAX1, respectively. It is possible that the formation of β-sheet, as monitored by CD, could result from the self-association of unfolded peptide. However, the incorporation of the strong β-turn-forming tetrapeptide (-V^{D}PPT-) into the sequence of MAX1 coupled with the observation that a control peptide (VKVKVKVK-NH_2) does not undergo gelation (vide infra) seems to suggest otherwise.

Infrared Spectroscopy. The existence of β-sheet structure within the hydrogel matrix is also supported by Fourier transform infrared (FTIR) spectroscopy (Figure 3). FTIR spectra of 1 wt % solutions of MAX1 at pH 5.5 display an amide I band at 1644 cm^{-1}, suggesting that the peptide is unfolded. Deuterium-exchanged peptides that adopt unordered conformations have been reported to display amide I bands at 1645 cm^{-1}.[52] However, when the pH of this solution is adjusted to 9.0 by the addition of NaOD, gelation occurs and the amide I band shifts to 1615 cm^{-1}, strongly suggesting that MAX1 adopts a structure rich in β-sheet. Typically, amide groups contained in β-structure give rise to bands ranging from 1620 to 1640 cm^{-1}. However, sheet-derived bands below 1620 cm^{-1} have been reported;[53] most notable is a sheet-rich aggregate of the peptide atriopeptin III.[54] The weak band at 1680 cm^{-1} suggests that the sheet structure may have some antiparallel character, or alternatively, this band could be attributed to β-turn structure.[55] The strong band at 1450 cm^{-1} evident in both spectra is most likely due to HOD bending and ND deformation.[56]

Rheology Studies. Bulk rheology experiments exhibit the manifestation of unimolecular folding and subsequent self-assembly into a gel network by the onset and growth of elastic properties. Figure 4a shows the results of a time sweep experiment at constant strain and frequency during which the growth of the storage modulus was monitored after hydrogelation was initiated for a 2 wt % solution of MAX1. Similar to the rate of β-sheet formation observed by CD (Figure 2b), rheology shows that the folding and assembly of MAX1 has significantly progressed after 30 min (gel storage modulus of ~600 Pa). Gel formation continued to mature after 2 h with a doubling of the gel modulus to ~1200 Pa. (The time sweep experiment was halted after 2 h due to concerns of water evaporation in the rheometer chamber.) An equilibrium storage modulus of ~1600 Pa was reached after several hours of gel formation; this equilibrium behavior is clearly shown by the linear, frequency-independent moduli measurements in Figure 4b. Rheological studies at lower peptide concentrations indicated that the crossover concentration separating a predominantly liquidlike ($G'' > G'$) vs a predominantly gellike ($G' > G''$) response is about 1 wt %. Several examples of hydrogel moduli from the literature are also shown in Figure 4b for comparison. The gel modulus of MAX1 is equal to, or larger than, any of these physically similar systems measured at similar concentration.

Two hallmarks of a self-assembled gel are exhibition of shear thinning and subsequent quick recovery of elastic properties after shearing has ended. Many physical gels, whether high molecular weight, hydrophilic polymer networks,[3,59−61] or self-assembled fibrillar,[62] membraneous,[7] and spherical micellular[63,64] gels, exhibit shear thinning behavior. This drop in viscosity (shear thinning) results from the disruption of any physical cross-links by the application of strain. Figure 4c clearly shows that MAX1-

(52) Surewicz, W. K.; Stepanik, T. M.; Szabo, A. G.; Mantsch, H. H. *J. Biol. Chem.* **1988**, *263*, 786−790.
(53) Surewicz, W. K.; Mantsch, H. H. *Biochim. Biophys. Acta* **1988**, *952*, 115−130.
(54) Surewicz, W. K.; Mantsch, H. H.; Stahl, G. L.; Epand, R. M. *Proc. Natl. Acad. Sci. U.S.A.* **1987**, *84*, 7028−7030.
(55) Surewicz, W. K.; Mantsch, H. H.; Chapman, D. *Biochemistry* **1993**, *32*, 389−394.
(56) Pastrana-Rios, B. *Biochemistry* **2001**, *40*, 9074−9081.
(57) Caplan, M. R.; Schwartzfarb, E. M.; Zhang, S. G.; Kamm, R. D.; Lauffenburger, D. A. *Biomaterials* **2002**, *23*, 219−227.
(58) Won, Y. Y.; Davis, H. T.; Bates, F. S. *Science* **1999**, *283*, 960−963.
(59) Owen, D. H.; Peters, J. J.; Katz, D. F. *Contraception* **2000**, *62*, 321−326.
(60) Xu, B.; Li, L.; Yekta, A.; Masoumi, Z.; Kanagalingam, S.; Winnik, M. A.; Zhang, K. W.; Macdonald, P. M. *Langmuir* **1997**, *13*, 2447−2456.
(61) Pelletier, E.; Viebke, C.; Meadows, J.; Williams, P. A. *Biomacromolecules* **2001**, *2*, 946−951.
(62) Terech, P. *Ber. Bunsen-Ges. Phys. Chem. Chem. Phys.* **1998**, *102*, 1630−1643.
(63) Prudhomme, R. K.; Wu, G. W.; Schneider, D. K. *Langmuir* **1996**, *12*, 4651−4659.
(64) Daniel, C.; Hamley, I. W.; Wilhelm, M.; Mingvanish, W. *Rheol. Acta* **2001**, *40*, 39−48.

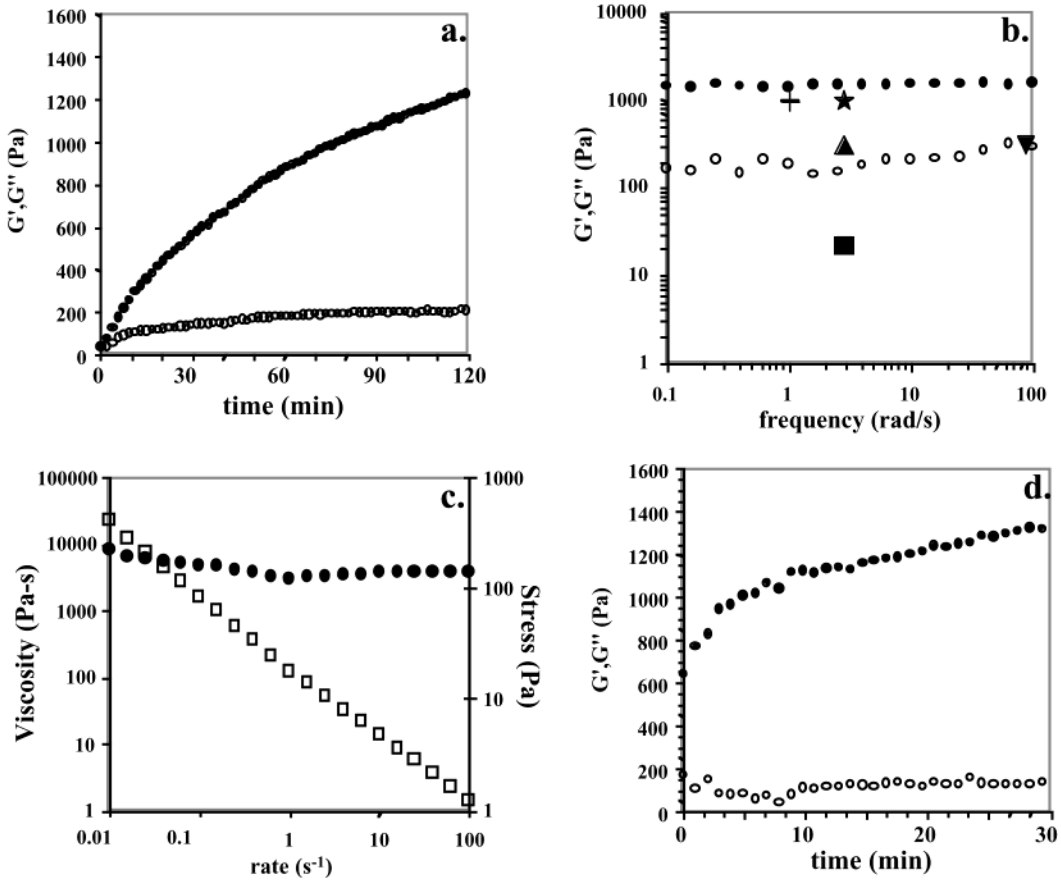

Figure 4. Rheology data on 2 wt % MAX1 hydrogel at pH 9. (a) Gel formation monitored as a function of time by increase in storage, G' (solid symbols), and loss, G'' (open symbols), shear moduli. (b) Frequency sweep data comparing moduli of MAX1 hydrogel to the storage moduli of representative self-assembled hydrogels from the literature: β-sheet by (+) Caplan et al.[57] and (★) Collier et al.;[17] (▲) fibrillar gel by Aggeli et al.;[18] (▼) coiled-coil proteinaceous gel by Petka et al.;[8] and (■) wormlike micelle gel by Won et al.[58] (c) Rate sweep data (viscosity, open symbols; stress, closed symbols) indicative of shear thinning material. (d) Restoration of gel moduli as a function of time after the cessation of strain treatment for gel network destruction (1000% strain at 6 Hz for 180 s). Symbols are as defined for panel a.

derived gels shear-thin; the viscosity drops with increasing strain rate. Importantly, unlike polymeric networks, self-assembled gels of MAX1 are capable of quickly reforming after cessation of shear due to the quick relaxation time of the molecular self-assembly process.[7] In Figure 4d, a time sweep experiment identical to that performed during the original gel formation was run immediately after the application of 1000% strain at 6 Hz for 180 s. The initial modulus of the reforming gel was 650 Pa, with 80% of the equilibrium modulus recovered after only 30 min, making this a quick recovering and relatively rigid hydrogel.

An interesting comparison can be made between the rheology data and the concentration-dependent CD data in Figure 2b. CD clearly shows that the rate at which MAX1 intramolecularly folds and self-assembles is positively dependent on peptide concentration. The rheologically monitored formation of the 2.0 wt % gel, approximately 6 mM in concentration, can be considered an analogous view of molecular folding and self-assembly at higher peptide concentrations (Figure 4a). Only after folding can the β-hairpin molecules self-assemble into a gel scaffold and thus provide a viscoelastic response. In fact, a control peptide that corresponds to the β-strand portions of MAX1 was synthesized (VKVKVKVK-NH_2). This peptide did not undergo hydrogelation when subjected to indentical folding conditions. Therefore, one directly observes the manifestation of molecular folding in the change of bulk material properties. A significant gel modulus (>100 Pa) is formed after only several hundred seconds, indicating a fast build-up of folded and assembled peptide. The processes continued over several hours with an increase of gel moduli (Figure 4a) that parallels a continued increase in sheet structure as monitored by CD (Figure 2b).

An analogous experiment examining the pH dependency of secondary structure as monitored by CD (Figure 2c) was accomplished with rheology to demonstrate that the gelation mechanism is reversible with pH changes. A small amount of concentrated HCl was added to a 2 wt % gel for a final approximate pH of 6.0. The system was thoroughly mixed by vigorous shaking for approximately 5 s and then immediately added to the rheometer chamber for a frequency sweep measurement. The rheological response of the system was essentially that of pure water, below the sensitivity threshold of the instrument, indicating a clear obviation of the self-assembled peptide scaffold and reversibility of gelation. This is in complete agreement with the immediate unfolding of MAX1 under acidic conditions as actively monitored via CD (Figure 2c). Therefore, CD experiments, which actively monitored the intramolecular folding and intermolecular sheet assembly of MAX1, and rheology experiments, which actively monitored the self-assembly of peptide into a gel scaffold, combine to form a clear image of how *material* properties can be attributed to *molecule* folding and consequent assembly mechanisms.

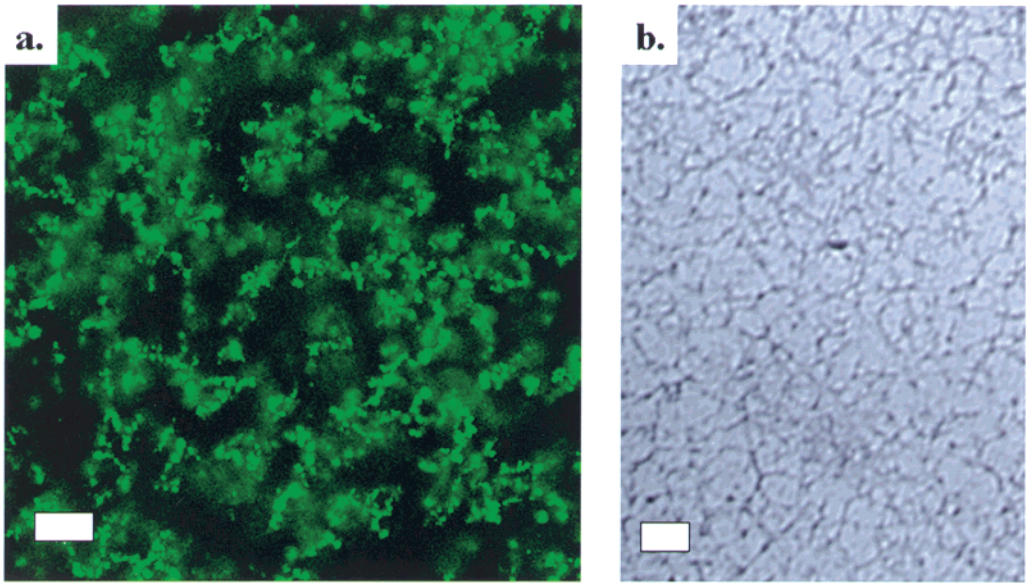

Figure 5. Microscopy of in situ gel morphology. (a) LSCM of hydrogel microstructure. Green regions are fluorescently stained self-assembled peptide, and black regions are water-filled pores and channels. Space bar = 20 μm. (b) CryoTEM of self-assembled scaffold nanostructure. Dark structures are self-assembled peptide scaffold, while lighter gray areas are composed of vitrified water. Space bar = 200 nm.

The pH responsiveness demonstrated here is an example of a triggered response in a material composed of self-assembled, designed peptides as proposed by Aggeli et al.[65] While a specific self-assembly mechanism is proposed by these authors for the formation of β-sheet-rich materials, further studies are needed to propose a detailed mechanism of the self-assembly process of MAX1 and its associated nanostructure.

Microscopy. The self-assembly mechanism leading to gel formation also manifests itself in the microscopic (Figure 5a) and nanoscopic (Figure 5b) morphology formed in the resultant material. Laser scanning confocal microscopy (LSCM) reveals a heterogeneous gel microstructure in which a continuous gel matrix is permeated by water channels. This innate heterogeneity has been observed in other self-assembled gel systems.[7] However, in traditional hydrogels prepared from cross-linked hydrophilic polymers, this microstructure must be processed into the material.[66−68] The gel matrix regions in Figure 5a are not solid peptide but rather a fibrillar/tubular network on the nanoscale that is itself permeated by water (Figure 5b). MAX1-derived gels are shear-thinning (Figure 4c) due to the ease of fracturing the assembled network structure and the dilute nature of the gel with regard to peptide. Also, the reversibility of the gelation process was again demonstrated by adding HCl to the hydrogels in the LSCM. The microstructure was immediately dissolved, presumably as a consequence of disassembly due to β-hairpin unfolding.

Small and Ultra-small Neutron Scattering. The combined SANS/USANS data for a 1 wt % gel in D_2O (Figure 6) further quantify the tubular/fibrillar structure of the gel matrix on the nanoscale and the heterogeneous morphology on the microscale. Scattering at low q clearly exhibits a slope of −4 (nonlinear, least-squares fit = −3.9) in log I vs log q, indicative of scattering from a sharp interface between two phases as described by Porod et al.[69] In this q regime the two phases are the gel matrix and the 1−10 μm sized water pores and channels, as clearly observed in the LSCM in Figure 5a. Therefore, the USANS data indicate a well-defined boundary on the micrometer length scale between the gel matrix and the water channels. In the SANS data at higher q, the most notable feature is the slope of approximately −1 in the Gunier region where the product of q and the radius of gyration, R_g, of a particle is <1.[70] [The inset in the upper right of Figure 6 is an enlargement of the log (intensity) from $0.02 < q < 0.08$ with a nonlinear, least-squares fit of −1.1.]

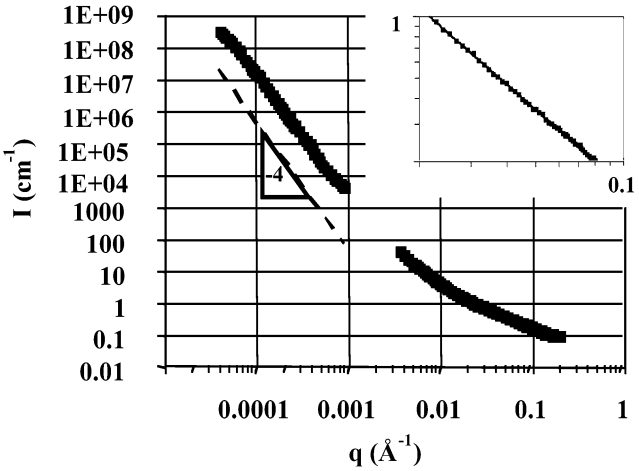

Figure 6. Combined USANS/SANS plot of 1 wt % MAX1 hydrogel formed in D_2O. The dashed line at lower q shows a slope of −4 in log (intensity) vs log (q) that represents theoretical scaling from scattering at a well-defined interface. These data indicate a sharp interface between the gel matrix and the water-filled channels on the microscale. (Inset) Expansion of higher q data ($0.02 < q < 0.1$) shows an approximate −1 slope in log (intensity) vs log (q) (fit slope = 1.18), suggesting rodlike structure on the nanoscale.

(65) Aggeli, A.; Nyrkova, I. A.; Bell, M.; Harding, R.; Carrick, L.; McLeish, T. C. B.; Semenov, A. N.; Boden, N. *Proc. Natl. Acad. Sci. U.S.A.* **2001**, *98*, 11857−11862.
(66) Mikos, A. G.; Thorsen, A. J.; Czerwonka, L. A.; Bao, Y.; Langer, R.; Winslow, D. N.; Vacanti, J. P. *Polymer* **1994**, *35*, 1068−1077.
(67) Martin, I.; Shastri, V. P.; Padera, R. F.; Yang, J.; Mackay, A. J.; Langer, R.; Vunjak-Novakovic, G.; Freed, L. E. *J. Biomed. Mater. Res.* **2001**, *55*, 229−235.
(68) Hassan, C. M.; Peppas, N. A. *J. Appl. Polym. Sci.* **2000**, *76*, 2075−2079.
(69) Porod, G. In *Small-Angle X-ray Scattering*; Glatter, O., Kratky, O., Eds.; Academic Press: London, 1982; pp 46−48.
(70) Guinier, A.; Fournet, G. *Small-Angle Scattering of X-rays*; Wiley-Interscience: New York, 1955.

This approximate scaling of -1 is indicative of scattering from a rodlike object on the nanoscale. This description is consistent with what can be observed in the cryoTEM data (Figure 5b), where the gel scaffold consists of either a fibrillar or tubular structure. Further neutron scattering work at more dilute concentrations where interparticle scattering can be faithfully neglected is required to more accurately determine the exact local structure of the β-hairpin assemblies, e.g., whether a classical β-sheet fibrillar structure exists[65,71] or a hollow, tubular structure[22] composes the gel scaffold.

Conclusions. Peptide design has been used to construct a chemically and mechanically responsive material. A peptide has been prepared that is incapable of ordered self-assembly under acidic solution conditions. However, in basic aqueous medium this sequence will adopt a β-hairpin conformation that is prone to self-assembly. Chemical responsiveness is realized by linking *intra*molecular folding and consequent *inter*molecular assembly to pH. Mechanical responsiveness is due to the self-assembled nature of the hydrogel scaffold. Designing peptides that intramolecularly fold on cue into a conformation prone to self-assembly may be a general design paradigm leading to responsive "smart" materials.

Experimental Section

General Methods and Materials. Trifluoroacetic acid (TFA), piperidine, thioanisole, ethanedithiol, boric acid, and anisole were purchased from Acros. Appropriately side-chain-protected Fmoc-amino acids, 2-(1*H*-benzotriazol-1-yl)-1,1,3,3-tetramethyluronium hexafluorophosphate (HBTU) and 1-hydroxybenzotriazole (HOBT) were purchased from Novabiochem. D_2O and NaOD were purchased from Cambridge Isotopes.

Peptide Synthesis. Peptides were prepared on Pal amide resin via automated Fmoc peptide synthesis employing an ABI 433A peptide synthesizer and HBTU/HOBT activation. The resulting dry resin-bound peptides were cleaved and side-chain-deprotected by use of TFA/thioanisole/ethanedithiol/anisole (90:5:3:2). Crude peptide was purified by RP-HPLC (preparative Vydac C4 peptide/protein column) employing a linear gradient from 12% to 100% B over 176 min, where solvent A is 0.1% TFA in water and solvent B is 90% acetonitrile, 10% water, and 0.1% TFA. After lyophilization, pure peptide was dissolved in water, resulting in a 100 μM solution, which was again lyophilized to ensure batch-to-batch consistency. MAX1, MS (MALDI-TOF) 2229.6 [$(M + H)^+$, calcd 2229.5]; Control peptide (VKVKVKVK-NH_2), MS (MALDI-TOF) 926.5 [$(M + H)^+$, calcd 926.7]. See Supporting Information for analytical HPLC and MS data for pure peptides.

Circular Dichroic Studies. CD spectra were collected at 25 °C on an Aviv model 215 spectropolarimeter. Time-dependent wavelength spectra of solutions of MAX1 (pH 9.0, 125 mM borate and 10 mM NaCl) were obtained in a 1 mm quartz cell. Peptide samples were prepared by diluting millimolar aqueous stock solutions with water to half the final volume; folding was initiated by an equal volume addition of a stock buffer solution (250 mM borate and 20 mM NaCl). Concentrations of peptide solutions were determined by absorbance at 220 nm ($\epsilon = 15\,750$ cm^{-1} M^{-1}). ϵ_{220} was determined by amino acid analysis. Mean residue ellipticity $[\theta]$ was calculated from the equation $[\theta] = (\theta_{obs}/10lc)/r$, where θ_{obs} is the measured ellipticity in millidegrees, l is the length of the cell (centimeters), c is the concentration (molar), and r is the number of residues. Base-induced folding (Figure 2c) was accomplished by adding 6 equiv of NaOH, and acid-induced unfolding was initiated by adding 10 equiv of HCl to a stirred aqueous solution of peptide; the pH was measured before and after each addition.

Infrared Spectroscopy. IR spectra were collected on a Nicolet Magna-IR 860 spectrometer employing a zinc-selenide flow cell. Soluble peptide samples were prepared by dissolving the deuteriochloride salt of solid MAX1 in D_2O, resulting in 1 wt % solution (pH 4.0, uncorrected). Hydrogel samples were prepared by titrating previously prepared deuterous solutions with NaOD until a solution pH of 9.0 (uncorrected) is reached with subsequent gelation. Deuterated MAX1*nDCl was prepared by lyophilizing the TFA salt of the peptide once from 0.1 M HCl and twice from D_2O.

Procedure for Hydrogel Preparation. Generally, basic solutions of MAX1 will undergo gelation at concentrations of 1 wt % or greater. Extremely uniform gels can be prepared according to the example procedure given below for the preparation of 300 μL of a 1 wt % hydrogel: To a solution of 3.0 mg of MAX1 in 150 μL of water was added 150 μL of a buffer stock solution (250 mM borate and 20 mM NaCl, pH 9.0), resulting in a 1 wt % solution (pH 9.0, 125 mM borate and 10 mM NaCl) of peptide. After minimal pipet mixing, this solution is allowed to stand for several hours until gelation is complete.

Rheology. Dynamic frequency, time, and strain sweep rheology experiments were performed on a Rheometrics Ares rheometer with a 25 mm diameter parallel plate geometry at 25 °C. Gel strength was monitored via frequency sweep measurements at fixed strain amplitude (1%) to measure the hydrogel storage, G', and loss, G'', moduli. Initial gel network formation of a 2 wt % solution (immediately after mixing an equal volume of an aqueous stock solution of peptide with an equal volume of stock buffer solution), gel recovery (after 1000% strain applied at 6 rad/s for 180 s to a preformed gel), and gel response to pH (immediately after addition of acid to stable gel) were monitored by observing G' and G'' at a constant frequency of 6 rad/s as a function of time. For shear thinning studies, gel viscosity was monitored as a function of strain rate.

Laser Scanning Confocal Microscopy. Hydrogels were imaged by use of a Zeiss 510 NLO microscope with an ArKr laser (30mW) at an excitation wavelength of 488 nm. Imaging of various *xy* planes within the sample was performed with an optical slice for all experiments of $\sim$1 μm. Lipophilic fluorescent dye (DiO C_{18}, Molecular Probes) was incorporated into the hydrogel scaffold by adding 50 μL of THF/dye solution (nanomolar concentration of dye) to an aqueous stock of peptide. Hydrogel formation was subsequently initiated by the equal volume addition of stock buffer solution (250 mM borate and 20 mM NaCl), resulting in a 1 wt % hydrogel. The dye was thus incorporated into the gel scaffold during peptide self-assembly to prevent nonuniform labeling of the hydrogel matrix that would otherwise occur if dye were added to a preformed gel due to limited solvent diffusion.

CryoTEM. Hydrogels were applied to carbon-coated copper grids with thicknesses $\sim$100 nm. The grids were plunged into liquid ethane cooled to -170 °C by use of a Leica EM CPS cryopreparation system actively cooled by liquid nitrogen. The vitrified samples, without further processing (e.g., staining or freeze-drying), were transferred under liquid nitrogen to a Gatan 626 cryoholder and cryotransfer system. During the observation of the samples in the microscope, the temperature of the holder was kept constant at -170 °C, preventing vitreous water sublimation. Images were taken in bright-field mode with a Jeol 2000 transmission electron microscope at 200 kV accelerating voltage. Structures were imaged while underfocused in order to enhance contrast.

SANS. Small-angle neutron scattering (SANS) experiments were performed on the 30-m instrument on beamline NG3 at the National Center for Neutron Research, National Institute of Standards and Technology, Gaithersburg, MD. The neutron beam was monochromated to 6 Å with a velocity selector having a wavelength spread of $\Delta\lambda/\lambda = 0.15$. The scattered neutrons were detected by a 64-cm $\times$ 64-cm two-dimensional detector with three different sample-to-detector distances, 13.1, 4.0, and 1.35 m. These configurations allow values of the scattering wavevector q in the range $0.004 < q$ (angstroms^{-1}) < 0.500. Here, q is the scattering vector defined as $q = (4/\lambda) \sin(\theta/2)$, where λ is the neutron wavelength (6 Å) and θ is the scattering angle. The

(71) Burkoth, T. S.; Benzinger, T. L. S.; Urban, V.; Morgan, D. M.; Gregory, D. M.; Thiyagarajan, P.; Botto, R. E.; Meredith, S. C.; Lynn, D. G. *J. Am. Chem. Soc.* **2000**, *122*, 7883−7889.

resulting data were corrected for background electronic noise and radiation, detector inhomogeneity, and empty cell scattering. Intensities were normalized to an absolute scale relative to main-beam transmission measurements through the sample. The uncertainties of the $I(q)$ versus q individual data points were calculated statistically from the number of averaged detector counts and are within the limits of the data point symbols.

USANS. Ultra-small-angle neutron scattering experiments (USANS) were performed on the perfect crystal diffractometer (PCD) on beam port BT-5 at the National Center for Neutron Research, National Institute of Standards and Technology, Gaithersburg, MD. Gel samples were housed in titanium sample cells with 30 mm diameter quartz windows and a 1 mm path length. β-Hairpin hydrogels for USANS were prepared in D_2O and NaOD base for adequate contrast between the hydrogen-rich gel scaffold matrix and the deuterated solvent. The USANS, Bonse Hart-type diffractometer, produces high q-resolution in one direction by using multiple reflections from silicon perfect crystals. A graphite premonochromator is used to select a 2.38 Å neutron wavelength beam. The beam is than diffracted by a three-bounce silicon (220) channel-cut monochromator. After the sample, another three-bounce channel-cut silicon crystal analyzer selects scattering at small angles (θ) in one direction. The data are slit-desmeared as described by Singh et al.[72]

Acknowledgment. This work was supported in part from the Petroleum Research Foundation (PRF36376-G4 and PRF35577-G7) and the NIH COBRE (P20 RR015588). We thank Professor Colin Thorpe and Professor Norman Wagner for thoughtful discussion.

Supporting Information Available: Analytical HPLC and MALDI-TOF mass spectrum of MAX1 and control peptide (2 pages, print/PDF). This information is available free of charge via the Internet at http://pubs.acs.org.

JA027993G

(72) Singh, M. A.; Ghosh, S. S.; Shannon, R. F. *J. Appl. Crystallogr.* **1993**, *26*, 787−794.